Desalination and Water Treatment
www.deswater.com

doi: 10.5004/dwt.2021.27238

227 (2021) 330–337
July

Enhanced photodegradation activity of cuprous oxide nanoparticles towards Congo red for water purification

Saba Rasheed[a], Zahida Batool[b], Azeem Intisar[c], Sara Riaz[d], Mamoona Shaheen[a], Rehana Kousar[a,*]

[a]*Lahore College for Women University, Lahore, Pakistan, emails: rehana2qandeel@hotmail.com (R. Kousar), sabarasheed200@gmail.com (S. Rasheed), mamoonashaheen689@gmail.com (M. Shaheen)*
[b]*The Islamia University of Bahawalpur, Bahawalpur, Pakistan, email: zahida.batool@iub.edu.pk*
[c]*The University of Punjab, Lahore, Pakistan, email: azeemintisar.chem@pu.edu.pk*
[d]*Comsats University Islamabad, Lahore Campus, Pakistan, email: sarahasnain@cuilahore.edu.pk*

Received 2 March 2020; Accepted 14 March 2021

ABSTRACT

Photocatalysis possesses enormous potential to facilitate the removal of environmental pollutants in the environment friendly ways. The nanostructured metal oxides have been found to show promising photocatalytic efficiencies toward organic pollutants. The present study deals with the synthesis of cuprous oxide and cupric oxide nanoparticles and characterization of their physiochemical, and photocatalytic properties using X-ray diffraction (XRD), scanning electron microscopy (SEM), Fourier transform infrared spectrometer (FT-IR), and UV-visible spectrometer. The as synthesized products were easily collected and purified and also tested for their photocatalytic activity toward water purification for removal of Congo red dye under sunlight. The impact of various factors on the catalytic efficiency of the synthesized nanoparticles, including catalyst concentration, reaction time, and pH of the solution has also been investigated. Both of these synthesized oxides of copper proved worthy of the said photocatalytic reaction and the results demonstrated an effective photodegradation of the Congo red under sunlight. It was found that Cu_2O possessed higher photodegradation efficiency of 90% as compared to 54% degradation efficiency of CuO.

Keywords: Cu_2O; CuO; Nanoparticles; Congo red; Photocatalytic activity; Water purification

1. Introduction

With the increase in population, industrialization, and the global economy, the world's environmental problems are increasing tremendously. Synthetic dyes are being employed in several industries, for example, textile, pharmaceutical, food, paper, cosmetic, and leather industries. The dye manufacturing industries produce about 7×10^5 metric tons of dyes per annum. During the dyeing process, not all the dye gets fixed on the fabric rather some unfixed dye gets washed out producing a large amount of liquid waste and the textile industry alone loses about 10%–25% of dyes during processing [1–4]. The release of these dyes in water is undesirable because of being toxic, mutagenic, and carcinogenic. Also, the demand and use of cotton are increasing nowadays. Mostly, azo dyes are used for dyeing of the cotton fibers. Due to their aromatic structure, most of the dyes are carcinogenic and possess acute and chronic toxicity, hence, they may cause skin irritation, allergies, dermatitis, or damage to tissues [5]. Also, to reuse the water, it is crucial to get a high degree of quality after the purification of wastewater. Various

* Corresponding author.

methods such as biological treatment, chemical, and adsorption have been used in the past to remove these dyes from water [6]. A new method that relies on the generation of hydroxyl radicals (•OH) named as advanced oxidative processes (AOPs) has proved the best method for the degradation of these organic pollutants. These hydroxyl radicals act as oxidizing agents and cause degradation of dyes, resulting in the formation of CO_2, H_2O, or some less toxic small molecule [4,7].

Semiconductor metal oxides have gained due interest owing to their applicability in various fields comprising of solar cells [8] water splitting [9], transistors [10], and photocatalysis [11,12]. The low-cost solution based techniques are employed to design the metal oxides. These semiconductor metal oxides at nanoscale exhibit higher environmental stability and superior charge carrier mobility as compared to other semiconductors including organic polymers. At the same time, they also possess special thermal, optical, physical, and chemical properties [13]. Moreover, the synthesis and design of metal oxide nanomaterials is an active area of research because of their uses as disinfectants, catalysts, semiconductors, and antimicrobial agents. Transition metals can form different oxides because of their ability to exhibit various oxidation states. These metal oxide nanoparticles in different oxidation states exhibit specific properties. One of the examples of an oxide system is that of copper which mainly exists in three forms Cu_4O_3, Cu_2O, and CuO [14,15]. Recently, Cu_2O nanostructures have become a subject of great interest owing to their good electronic performance, electrochemical properties, superconductivity, low toxicity, and low cost [16–18]. Some Cu_2O nanostructures have specific applications among electronic printing [12], lithium-ion batteries [19], sensors [20], and photocatalysis [21]. Cu_2O has also been proved better material for removing Organic dyes from water [22]. On the other hand, important properties of cupric oxide (CuO) nanoparticles such as thermal stability and optical properties inspired the other researchers to investigate this material for electrical conductivity and photocatalytic activity [19,23]. The nanosize CuO finds its most salient application in solar energy and electrical energy storage batteries [24,25]. Copper oxide (Cu_2O and CuO) nanoparticles have been synthesized through various methods including microwave irradiation [26], vapor deposition [27], thermal decomposition [28], electrochemical [17], and green/biosynthetic methods [29] as well.

As the industrial effluents add harmful effects to water streams, a strong need exists to design the materials and processes that aid to purify and limit the dye products in water. Hence, in the current work, efforts have been devoted to prepare catalysts having high photocatalytic activity, low toxicity, and visible light activity. Literature has reported the synthesis of several visible-light-driven photocatalysts. One of the most important achievements is the synthesis of Cu_2O and CuO nanoparticles as these nanoparticles have narrow band gaps of 2.2 eV [15] and 1.2 eV [30], respectively. In literature, work has reported the degradation of various organic dyes including salicylic acid [31], p-nitrophenol [30], Acid Black 210 [32], and Rhodamine B [33] Methylene blue, Methyl orange [22] using CuO and Cu_2O nanoparticles as a catalyst but up till now, the degradation of Congo red has not been studied toward the impact of the metal oxidation state of the photocatalyst.

In the present work, we reported the successful synthesis of Cu_2O and CuO nanoparticles by an easy and cost-effective solution method. Moreover, these synthesized oxides of Copper (Cu_2O and CuO) were employed toward photodegradation of an azo dye (Congo red) in aqueous solution. Cong red (azo dye) is being employed in textile industries, released into the water bodies, and causes serious health problems to humans because of being mutagenic and carcinogenic. The various factors that can affect the photocatalytic activity of nanoparticles have also been investigated.

2. Materials and methods

The chemicals required for this study were purchased from the Sigma Aldrich. These were of high purity, so no further purification was performed. All of the experiments were carried out using distilled water.

2.1. Synthesis of Cu_2O and CuO nanoparticles

Cuprous and cupric oxide nanoparticles were prepared using copper chloride as the main precursor. Ascorbic acid, trisodium citrate, and sodium hydroxide were also used during the synthesis. Briefly, in 100 mL of distilled water, the corresponding amounts in grams of trisodium citrate (0.25 M) and that of ascorbic acid (0.04 M) were added. Ascorbic acid functions as a stabilizing agent during the synthesis process. This solution was heated to boiling with constant stirring. To this heated solution, 50 mL solution of copper chloride (0.5 M) was added drop wise (in half an hour) under constant stirring. The formation of yellowish-orange particles was observed on the addition of 50 mL of 2 N NaOH, marking the onset of Cu_2O nanoparticles. These particles were collected by filtration and washed several times using distilled water and ethanol. These synthesized Cu_2O nanoparticles were subjected to drying in an oven at 90°C for 24 h. For the synthesis of CuO nanoparticles, the same procedure was followed but the yellowish-orange particles were not separated immediately and kept for 48 h. The color of particles changed from yellowish-orange to brown-black color, marking the onset of CuO nanoparticles. These particles were also collected after filtration and washed several times using distilled water and ethanol. These synthesized CuO nanoparticles were also dried at 90°C for 24 h.

2.2. Characterization of synthesized Cu_2O and CuO nanoparticles

The synthesized Cu_2O and CuO nanoparticles were subjected to structural characterization by UV-visible, FT-IR, and XRD analysis. For UV-visible study, the synthesized materials were dispersed in deionized water in the form of thin films, and absorbance was recorded. The XRD analysis was performed using Cu Kα radiations with a speed of 0.05°/s. The morphological study of Cu_2O and CuO nanoparticles was carried out by scanning electron microscopy (SEM) using EVO LS 10.

2.3. Photocatalytic activity of Cu_2O and CuO nanoparticles

To evaluate the photocatalytic activity associated with the synthesized copper oxides, these were employed toward Congo red degradation by UV-visible absorption technique. For this purpose, 10 mg/L of Congo red (aqueous solution) was prepared and the volume of the solution was set to 100 mL. The absorbance of the solution without nanoparticles (blank samples) was recorded using a UV/Vis spectrophotometer. 10 mg of Cu_2O and 10 mg of CuO nanoparticles were added to separate containers with 100 mL of 10 mg/L solution of the dye in dark and stirred for 30 min. to reach an adsorption/desorption equilibrium. Later, both of these solutions were kept in sunlight and the absorbance of solutions was recorded after successive time intervals of every 15 min. The following formula was used to calculate the dye degradation efficiency of these oxides:

$$\% \text{ degradation} = \frac{A-B}{A} \times 100 \quad (1)$$

where A and B represent the absorbance of dye solution without catalyst and with catalyst, respectively.

3. Results and discussion

3.1. Characterization

Fig. 1 shows the UV-visible spectra for oxides of copper recorded in the range of 200–800 nm. The maximum absorption peak at 505 nm corresponds to Cu_2O nanoparticles [34] and the maximum absorption peak at 385 nm corresponds to CuO nanoparticles [33].

Fig. 2 displays the FT-IR spectra of oxides of copper recorded from 450 to 1,500 cm^{-1}. An FT-IR spectrum is a quite helping tool for analyzing the metal oxide as it gives useful information about their nature. Metal oxides generally show peaks below 1,000 cm^{-1} [31]. The characteristic peak at 605 cm^{-1} corresponds to Cu_2O nanoparticles and the peaks at 478 and 547 cm^{-1} correspond to CuO nanoparticles [35].

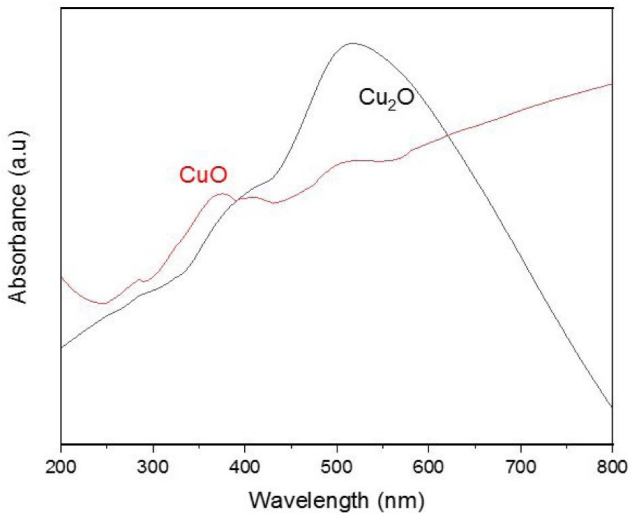

Fig. 1. UV-vis spectra of Cu_2O and CuO nanoparticles.

3.2. X-ray diffraction analysis

Further characterization of the synthesized oxides of copper was performed using X-ray diffraction (XRD). Fig. 3 gives the XRD patterns of Cu_2O and CuO nanoparticles. A prominent difference could be noted in the recorded XRD spectra of both Cu(I) and Cu(II) oxides. The peaks for CuO are comparatively broader as compared to that of Cu_2O and this broadening could be because of the smaller particle size of CuO nanoparticles than that of Cu_2O. The two most sharp diffraction peaks at 35.5 and 38.7 were observed for CuO. The other small peaks for CuO include 2θ values at 32.5°, 48.7°, 53.5°, 58.5°, 61.5°, 66.3°, and 68.05°. Whereas, for Cu_2O, the three most intense peaks were observed at 36.3°, 42.3°, and 61.4°. The other small peaks include at 29.5° and 73.5°. The corresponding hkl values of these peaks have been given in Table 1. [36,37]. The average particle size of the Cu_2O and CuO was calculated to be 12.00 and 9.65 nm, respectively. Three most intense peaks were selected to calculate the particle sized using Debye–Scherer's formula:

$$D = \frac{K\lambda}{\beta \cos\theta} \quad (2)$$

3.3. SEM observation

The morphology of synthesized Cu_2O and CuO nanoparticles was examined by SEM and is given in Fig. 4. The SEM images reveal that both the Cu_2O and CuO nanoparticles have a spherical shape. Fig. 4a reveals that Cu_2O nanoparticles are connected, while Fig. 4b shows that in the case of CuO, a low interconnection among nanoparticles as that of Cu_2O is observed.

The synthesis of Cu_2O and CuO from precursor involves the formation of the copper-citrate complex as an intermediate during the reaction. This copper–citrate complex is reduced by sodium hydroxide and results in the formation of Cu_2O nanoparticles. These Cu_2O nanoparticles undergo oxidation resulting in the generation of CuO nanoparticles through direct oxidation or the formation of $Cu(OH)_2$.

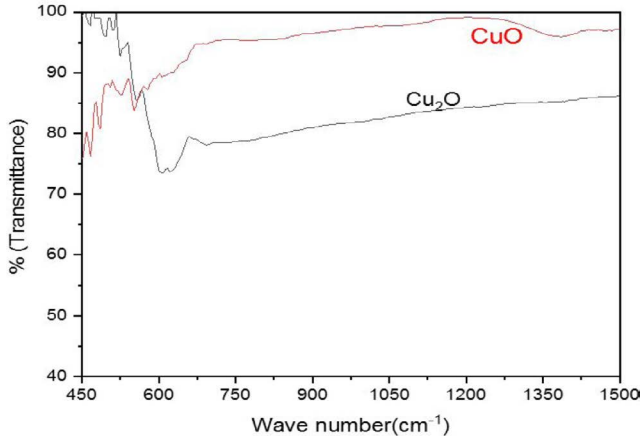

Fig. 2. FT-IR spectra of Cu_2O and CuO nanoparticles.

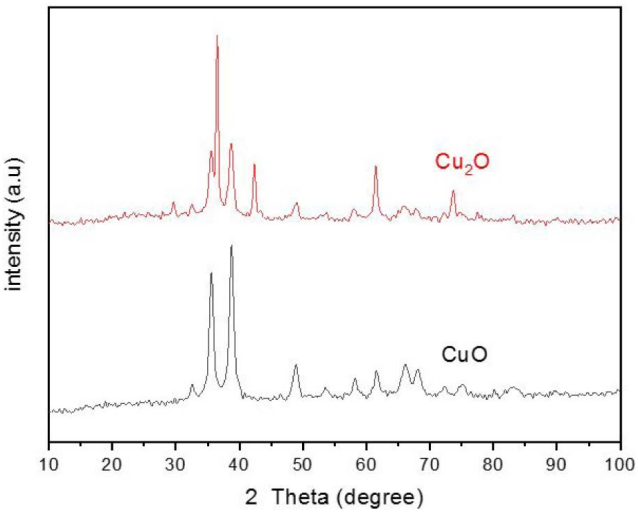

Fig. 3. XRD patterns of Cu_2O and CuO nanoparticles.

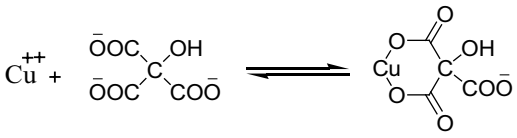

(3)

$$Cu\text{-}(Citrate)^{-1} + NaOH \rightarrow Cu_2O \quad (4)$$

$$Cu_2O + 2OH^- \rightarrow 2CuO + H_2O \quad (5)$$

$$Cu_2O + H_2O + 2OH^- \rightarrow 2Cu(OH)_2 \quad (6)$$

$$Cu(OH)_2 \rightarrow CuO + H_2O \quad (7)$$

Fig. 4a is the synthesis scheme of copper oxides.

Cuprous and cupric oxide nanoparticles possess catalytic activity toward dye degradation and they are used to remove the organic dyes from water. The possible mechanism of CR degradation in the presence of synthesized copper oxides and visible light irradiation is as follows. The excitation by visible light leads to absorption of photons (with higher energy than metal oxide band gap) on the surface of metal oxide particles. As a consequence, electrons from the valence band (VB) are excited to conduction band (CB) generating electrons (e^-) in the CB and hole (h^+) in the VB, as shown in Fig. 5. In the next step, the electrons react with O_2 molecule and produce $O_2^{-\bullet}$, that is, super oxide ions. The holes (h^+) react OH– from water (H_2O) to produce $OH^\bullet$ free radicals. Finally, these generated free radicals can interact with the pollutant (CR) molecules to convert it to nontoxic degradation products. The disintegration of organic dye (Congo red) by the metal oxide nanoparticles is shown in Fig. 5.

Table 1
XRD data of synthesized copper oxides

CuO		Cu_2O	
Observed 2θ	hkl	Observed 2θ	hkl
32.5	110	29.5	110
35.5	–111	36.3	111
38.7	111	42.3	200
48.7	–202	61.4	220
53.5	020	73.5	311
58.3	202		
61.5	–113		
66.3	–311		
68.05	220		

3.4. Photocatalytic test

The photocatalytic activity of synthesized Cu_2O and CuO nanoparticles was studied at a wavelength of

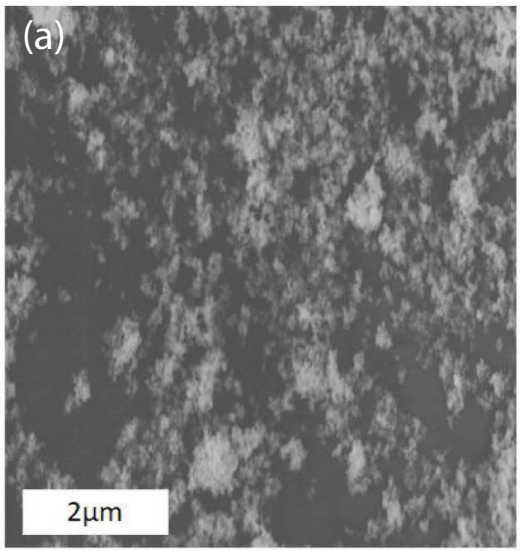

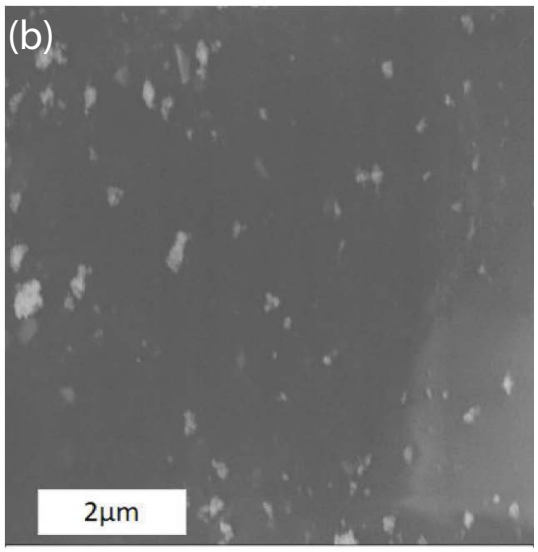

Fig. 4. SEM analysis of (a) Cu_2O and (b) CuO nanoparticles.

495 nm (λ_{max}). This wavelength was chosen for analyzing the degradation activity because the Congo red showed λ_{max} at a wavelength of 495 nm. UV-vis spectrum of Congo red is shown in Fig. 6. To investigate the photocatalytic degradation of Congo red concerning time, several experiments were carried out and the degradation phenomenon was studied at different time intervals. A blank experiment comprising the photocatalytic degradation of the dye solution without a catalyst was designed. In another set of experiments, the photocatalytic degradation of the dye solution was examined using the catalyst. Absorbance was recorded and the % degradation was calculated. It was noted that in the absence of catalysts the dye solution does not undergo photocatalytic degradation effectively. While in the presence of catalysts the dye solution undergoes degradation effectively. CuO nanoparticles showed maximum degradation at 2 h of exposure with 54% degradation while Cu_2O nanoparticles showed a maximum degradation at 3 h of exposure with 90% degradation. The % degradation of Congo red at various time intervals is shown in Fig. 7a. A brief comparison of the current work with that of reported in the literature is given in Table 2.

The % degradation of Congo red at different concentrations of Cu_2O and CuO nanoparticles (0.01–0.05 g) in 10 mg/L (100 mL) dye solution was studied for a duration of 2 h exposure to sunlight. It was observed that Congo red undergoes degradation with both of the synthesized catalysts. As the concentration of Cu_2O nanoparticles increases, the % degradation remains almost constant but an increase in the degradation activity was noted with an increasing amount of the CuO nanoparticles. The % degradation of Congo red at different concentrations of Cu_2O and CuO nanoparticles is given in Fig. 7b. The turn over frequency (TOF) of the prepared structures was also calculated and has been given in Fig. 7d.

The industrial water is not necessarily neutral and may be acidic or basic, depending upon the specific circumstances. Moreover, the pH of the dye solution also affects the degradation efficiency of the catalysts. The % degradation of Congo red at different pH of the dye solution was investigated at a reaction duration of 2 h using synthesized copper oxide nanoparticles and is shown in Fig. 7c. It was noted that both the synthesized Cu_2O and CuO nanoparticles show 100% degradation at pH = 2. The concept of point zero charges (pH_{ZPC}) can explain these results. The point of zero charge is a condition when a

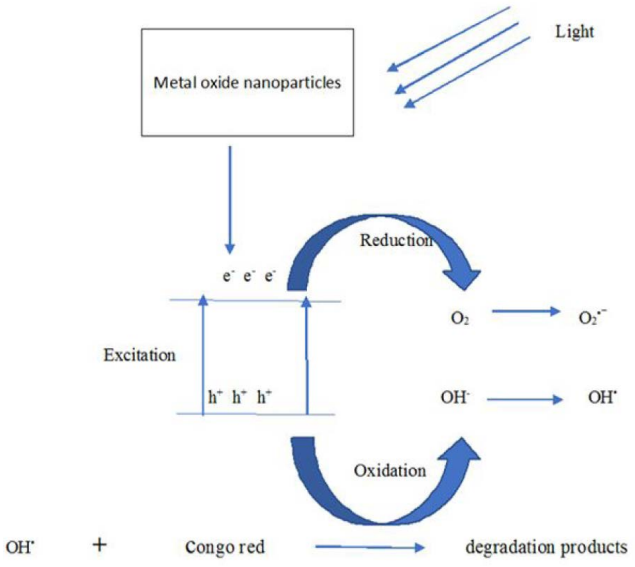

Fig. 5. Photocatalytic activity of metal oxide nanoparticles.

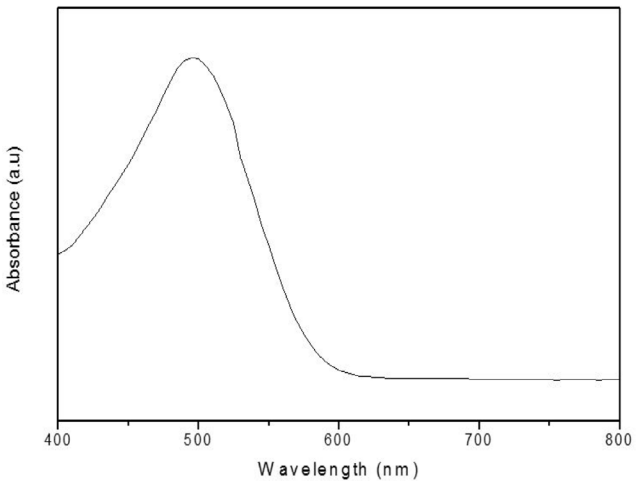

Fig. 6. UV-vis spectrum of Congo red.

Table 2
Brief summary of the literature on the photodegradation of Congo red by metal oxides

Catalyst	Synthetic method	Catalyst loading	Initial dye concentration	Light source	Time (min)	% degradation	Ref.
ZnO	Co-precipitation	0.5 g/L	20 mg/L	Solar simulator	120	85	[41]
WO_3	Solution method	–	15 mg/L	Visible light (Xenon lamp)	60	86	[42]
ZnO	Obtained from Merck	0.5 g/L	20 mg/L	UV	60	95.02	[43]
TiO_2	–	0.5 g/L	20 mg/L	UV	60	93.0	[43]
CuO	Biosynthesis	0.05 g/50 mL	10 mg/L	Sunlight	60	88.0	[44]
CuO	Direct oxidation	0.1 g/100 mL	20 mg/L	UV	210	75	[45]
CuO	Solution method	0.01 g/100 mL	10 mg/L	Sunlight	120	100	This work

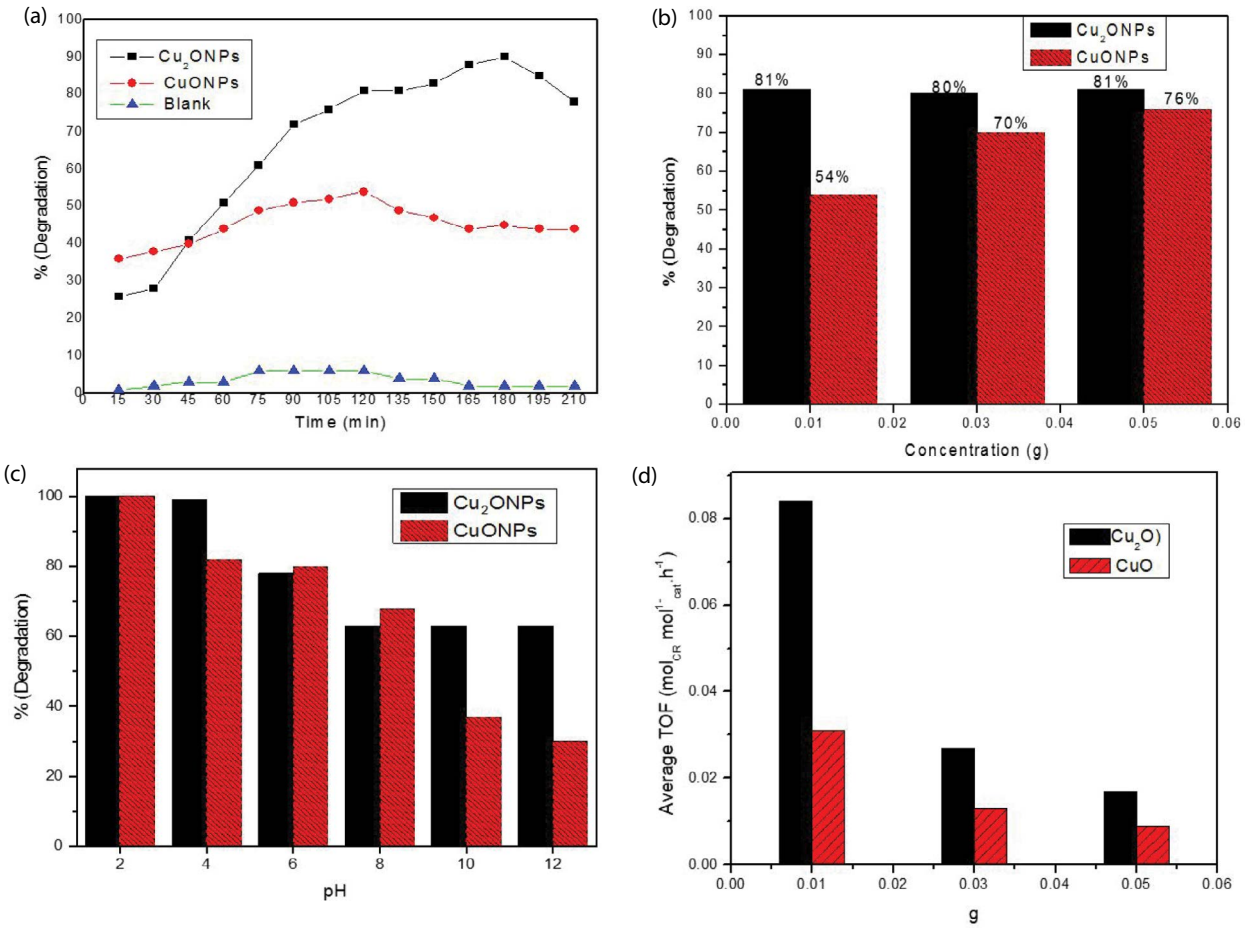

Fig. 7. % Degradation of Congo red at (a) various time intervals, (b) different concentrations of Cu_2O and CuO nanoparticles, (c) pH at exposure time of 2 h, and (d) TOF of the prepared structures.

substance possesses a zero-surface density. The pH higher than the pH_{ZPC} value indicates that the catalyst surface has been negatively charged. Whereas, a pH lower than pH_{ZPC} value indicates that the catalyst surface has been positively charged [38]. In literature, the pH_{ZPC} for Cu_2O and CuO nanoparticles was found to be at pH of 8–8.2 and 7.6–9.8, respectively [39,40]. Moreover, the Congo red is an azo dye carrying a negative charge. At a pH value lower than their pH_{ZPC}, a higher degradation activity of the catalyst is resulted because of a strong electrostatic field between the positively charged catalyst material and negatively charged Congo red. It was also observed that with a decrease in pH of the dye solution, from 12 to 8, the catalytic efficiency of Cu_2O nanoparticles remained constant with 63% degradation. While from pH 8 to 2 catalytic efficiency of Cu_2O increased from 63 to 100%. On the other hand, CuO nanoparticles showed a continuous increase in their catalytic efficiency with a decrease in pH of the dye solution from 12 to 2. With a change in pH of the dye solution from 12 to 2, the catalytic efficiency of CuO increased from 30% to 100%.

4. Conclusion

Both Cu_2O and CuO nanoparticles proved worthy of degradation of Congo red in aqueous solution under visible light. Moreover, the existence of Cu in +1 and +2 oxidation states in the synthesized nanoparticles affect their catalytic activity. CuO nanoparticles showed maximum degradation (54%) at an exposure time of 2 h and after this time its degradation was not affected while Cu_2O nanoparticles showed maximum degradation (90%) at an exposure time of 3 h. There was no effect of concentration of Cu_2O nanoparticles on the % degradation of Congo red but as the concentration of CuO nanoparticles was increased, the % degradation of the dye increases. The pH of the dye solution also affected the catalytic efficiency of the synthesized oxides of the Copper. With a decrease in pH of the dye solution, from 12 to 8, the catalytic efficiency of Cu_2O nanoparticles remained constant with 63% degradation. While from pH 8 to 2 catalytic efficiency ofCu_2O increased from 63 to 100%. On the other hand, CuO nanoparticles showed a continuous increase in their catalytic efficiency with a decrease in pH of the dye solution from 12 to 2. With a change in pH of the dye solution from 12 to 2, the catalytic efficiency of CuO increased from 30% to 100%.

References

[1] A. Baban, A. Yediler, N.K. Ciliz, Integrated water management, and CP implementation for wool and textile blend processes, Clean Soil Air Water, 38 (2010) 84–90.

[2] T. Robinson, G. Mcmullan, R. Marchant, P. Nigam, Remediation of dyes in textile effluent: a critical review on current treatment technologies with a proposed alternative, BioresTech, 77 (2001) 247–255.
[3] P.A. Soloman, C.A. Basha, M. Velan, V. Ramamurthi, K. Koteeswaran, N. Balasubramanian, Electrochemical degradation of Remazol Black B dye effluent, Clean Soil Air Water, 37 (2009) 889–900.
[4] K.O. Badmus, J.O. Tijani, E. Massima, L. Petrik, Treatment of persistent organic pollutants in wastewater using hydrodynamic cavitation in synergy with advanced oxidation process, Environ. Sci. Pollut. Res., 25 (2018) 7299–7314.
[5] H. Börnick, T.C. Schmidt, Amines, T. Reemtsma, M. Jekel, Eds., Organic Pollutants in the Water Cycle: Properties, Occurrence, Analysis, and Environmental Relevance of Polar Compounds, Wiley-VCH Verlag GmbH & Co. KGaA, Weinheim, 2006, pp. 181–208.
[6] A. Kumar, G. Pandey, Photocatalytic degradation of Eriochrome Black-T by the Ni:TiO_2 nanocomposites, Desal. Water Treat., 71 (2017) 406–419.
[7] M. Hua, X. Wanga, H. Liua, N. Lia, T. Lib, R. Zhang, D. Chena, Visible-light-driven photodegradation of aqueous organic pollutants by Ag/AgCl@$Zn_3V_2O_8$ nanocomposites, Desal. Water Treat., 86 (2017) 102–114.
[8] S. Brittman, Y. Yoo, N.P. Dasgupta, S.i. Kim, B. Kim, P. Yang, Epitaxically aligned cuprous oxide nanowires for all-oxide, single-wire solar cells, Nano Lett., 14 (2014) 4665–4670.
[9] Y.H. Zhang, B.B. Jiu, F.L Gong, J.L. Chen, H.L. Zhang, Morphology controllable Cu_2O supercrystals: facile synthesi, facet etching mechanism and comparative photocatalytic H_2 production, J. Alloys Compd., 729 (2017) 563–570.
[10] X. Yu, T.J. Marks, A. Facchetti, Metal oxides for optoelectronic applications, Nat. Mater. 15 (2016) 383–396.
[11] M. Kumar, R.R. Das, M. Samal, K. Yun, Highly stable functionalized cuprous oxide nanoparticles for photocatalytic degradation of methylene blue, Mat. Chem. Phys., 218 (2018) 272–278.
[12] F. Zhang, G. Dong, M. Wang, Y. Zeng, C. Wang, Efficient removal of methyl orange using Cu_2O as a dual function catalyst, Appl. Surf. Sci., 444 (2018) 559–568.
[13] M.A. El-Sayed, Some interesting properties of metals confined in time and nanometer space of different shapes, Acc. Chem. Res., 34 (2001) 257–264.
[14] E. Roduner, Size matters: why nanomaterials are different, Chem. Soc. Rev., 35(2006) 583–592.
[15] B.K. Meyer, A. Polity, D. Reppin, M. Becker, P. Hering, P.J. Klar, T. Sander, C. Reindl, J. Benz, M. Eickhoff, C. Heiliger, M. Heinemann, J. Bläsing, A. Krost, S. Shokovets, C. Müller, C. Ronning, Binary copper oxide semiconductors: from materials towards devices, Phys. Status Solid B, 249 (2012) 1487–1509.
[16] W.-R. Lee, Y.S. Lim, S. Kim, J. Jung, Y.-K. Han, S. Yoon, L. Piao, S.H. Kim, Crystal-to-crystal conversion of Cu_2O nanoparticles to Cu crystals and applications in printed electronics, J. Mater. Chem., 21 (2011) 6928–6933.
[17] Y.-K. Hsu, C.-H. Yu, Y.-C. Chen, Y.-G. Lin, Hierarchical Cu_2O photocathodes with nano/microspheres for solar hydrogen generation, RSC Adv., 2 (2012) 12455–12459.
[18] B. Li, H. Cao, G. Yin, Y. Lu, J. Yin, Cu_2O@reduced graphene oxide composite for removal of contaminants from water and supercapacitors, J. Mater. Chem., 21 (2011) 10645–10648.
[19] J.H. Shin, S.H. Park, S.M. Hyun, J.W. Kim, H.M. Park, J.Y. Song, Electrochemical flow-based solution–solid growth of the Cu_2O nanorod array: potential application to lithium-ion batteries, PhysChem. Chem. Phys., 16 (2014) 18226–18232.
[20] J. Zhang, J. Liu, Q. Peng, X. Wang, Y. Li, Nearly Monodisperse Cu_2O and CuO Nanospheres: preparation and applications for sensitive gas sensors, Chem. Mater., 18 (2006) 867–871.
[21] H. Yang, J. Ouyang, A. Tang, Y. Xiao, X. Li, X. Dong, Y. Yu, Electrochemical synthesis and photocatalytic property of cuprous oxide nanoparticles. Mater Res. Bull., 41 (2006) 1310–1318.
[22] J. Shi, J. Li, X. Huang, Y. Tan, Synthesis, and enhanced photocatalytic activity of regularly shaped Cu_2O nanowire polyhedral, Nano Res., 4 (2011) 448–459.
[23] A. Bhattacharjee, S. Begum, K. Neog, M. Ahmaruzzaman, Facile synthesis of 2D CuO nano leaves for the catalytic elimination of hazardous and toxic dyes from aqueous phase: a sustainable approach, Environ. Sci. Pollut. Res., 23 (2016) 11668–11676.
[24] A. Rakhshani, Preparation, characteristics, and photovoltaic properties of cuprous oxide—a review, Solid-State Electron., 29 (1986) 7–17.
[25] H. Wang, Q. Pan, J. Zhao, W. Chen, Fabrication of CuO/C films with sisal-like hierarchical microstructures and its application in lithium-ion batteries, J. Alloys Compd., 476 (2009) 408–413.
[26] Y. Zhao, J.-J. Zhu, J.-M. Hong, N. Bian, H.-Y. Chen, Microwave-induced polyol-process synthesis of copper and copper oxide nanocrystals with controllable morphology, Eur. J. Inorg. Chem., 2004 (2004) 4072–4080.
[27] Z. Liu, Y. Bando, A novel method for preparing copper nanorods and nanowires, Adv. Mater., 15 (2003) 303–305.
[28] N.A. Dhas, C.P. Raj, A. Gedanken, Synthesis, characterization, and properties of metallic copper nanoparticles, Chem. Mater., 10 (1998) 1446–1452.
[29] B.T. Sone, A. Diallo, G. Fukua, A. Gurib-Fakim, M. Maaza, Biosynhesized CuO nano-platelets: physical properties & enhanced thermal conductivity nanofluidics, Arabian J. Chem., 13 (2020) 160–170.
[30] A. Bhattacharjee, M. Ahmaruzzaman, CuO nanostructures: facile synthesis and applications for enhanced photodegradation of organic compounds and reduction of p-nitrophenol from the aqueous phase, RSC Adv., 6 (2016) 41348–41363.
[31] M.M. Momeni, M. Mirhosseini, Z. Nazari, A. Kazempour, M. Hakimiyan, Antibacterial and photocatalytic activity of CuO nanostructure films with different morphology, J. Mater. Sci. – Mater. Electron., 27 (2016) 8131–8137.
[32] F. Ijaz, S. Shahid, S.A. Khan, W. Ahmad, S. Zaman, Green synthesis of copper oxide nanoparticles using *Abutilon indicum* leaf extract: antimicrobial, antioxidant and photocatalytic dye degradation activities, Trop. J. Pharm. Res., 16 (2017) 743–753.
[33] L.J. Xie, W. Chu, J.H. Sun, P. Wu, D.G. Tong, Synthesis of copper oxide vegetable sponges and their antibacterial, electrochemical and photocatalytic performance, J. Mater. Sci., 6 (2011) 2179–2184.
[34] S.S. Sawant, A.D. Bhagwat, C.M. Mahajan, Synthesis of cuprous oxide (Cu_2O) nanoparticles – a review, J. Nano Electron. Phys., 8 (2016), doi: 10.21272/jnep.8(1).01035.
[35] J. Santhanalakshmi, V. Dhanalakshmi, Synthesis, size characterization, and catalytic application studies on the biostabilised CuO nanocubes for the oxidation of drugs with pH and mass effects, Int. J. Sci. Res. Pub., 12 (2012) 1–10.
[36] A. Abdulkarem, E.A. Ammar, Y. Ying, L.J. Lin, Preparation of Cu_2O from TiO_2 and CTAB using the anode support system, J. Appl. Sci., 8 (2008) 4674–4678.
[37] R. Raghav, P. Aggarwal, S. Srivastava, Tailoring oxides of copper-Cu_2O and CuO nanoparticles and evaluation of organic dyes degradation, AIP Conf. Proc., 1724 (2016), doi: 10.1063/1.4945198.
[38] A.C. Bertoli, R. Carvalho, M.P. Freitas, T.C. Ramalho, D.T. Mancini, M.C. Oliveira, A.d. Varennes, A. Dias, Structural determination of Cu and Fe–Citrate complexes: theoretical investigation and analysis by ESI-MS, J. Inorg. Biochem., 144 (2015) 31–37.
[39] D. Wang, M. Mo, D. Yu, L. Xu, F. Li, Y. Qian, Large-scale growth and shape evolution of Cu_2O cubes, Cryst. Growth Des., 3 (2003) 717–720.
[40] I. Zaafarany, H. Boller, Electrochemical behavior of copper electrode in sodium hydroxide solutions, Curr. World Environ., 4 (2009) 277–284.
[41] R.E. Adam, G. Pozina, M. Willander, O. Nur, Synthesis of ZnO nanoparticles by co-precipitation method for solar driven photodegradation of congo red dye at different pH, Photonics Nanostruct. Fundam. Appl., 32 (2018) 11–18.
[42] S.V. Prabhakar Vattikuti, C. Byon, I. Ngo, Highly crystalline multilayered WO_3 sheets for photodegradation of congo red

under visible light irradiation, Mater. Res. Bull., 84 (2016) 288–297.
[43] L. Nadjia, E. Abdelkader, B. Ahmed, Photodegradation study of Congo Red in aqueous solution using ZnO/UV-A: effect of pH and band gap of other semiconductor groups, J. Chem. Eng. Process. Technol., 2 (2011) 1–9.
[44] M. Aminuzzaman, L.M. Kei, W.H. Liang, Green synthesis of copper oxide (CuO) nanoparticles using banana peel extract and their photocatalytic activities, AIP Conf. Proc., 1828 (2017), doi: 10.1063/1.4979387.
[45] M. Farbod, N.M. Ghaffari, I. Kazeminezhad, Effect of growth parameters on photocatalytic properties of CuO nanowires fabricated by direct oxidation, Mater. Lett., 81 (2012) 258–260.